Time-resolved x-ray absorption spectroscopy: Watching atoms dance

2009 J. Phys.: Conf. Ser. 190 012052

(http://iopscience.iop.org/1742-6596/190/1/012052)

Journal of Physics: Conference Series **190** (2009) 012052 doi:10.1088/1742-6596/190/1/012052

Time-resolved x-ray absorption spectroscopy: Watching atoms dance

Chris J. Milne[1], Van-Thai Pham[1], Wojciech Gawelda[3], Renske M. van der Veen[1,2], Amal El Nahhas[1], Steven L. Johnson[2], Paul Beaud[2], Gerhard Ingold[2], Frederico Lima[1], Dimali A. Vithanage[1], Maurizio Benfatto[4], Daniel Grolimund[2], Camelia Borca[2], Maik Kaiser[2], Andreas Hauser[5], Rafael Abela[2], Christian Bressler[6], and Majed Chergui[1]

[1]Laboratoire de Spectroscopie Ultrarapide, Ecole Polytechnique Fédérale de Lausanne, Switzerland
[2] Swiss Light Source, Paul Scherrer Institut, Switzerland
[3] Laser Processing Group, Instituto de Óptica, CSIC, Spain
[4] Laboratori Nazionali di Frascati, INFN, Italy
[5] Département de Chimie Physique, Université de Genève, Switzerland
[6] European XFEL Project Team, Deutsches Elektronen Synchrotron, Germany

E-mail: majed.chergui@epfl.ch, chris.milne@psi.ch

Abstract. The introduction of pump-probe techniques to the field of x-ray absorption spectroscopy (XAS) has allowed the monitoring of both structural and electronic dynamics of disordered systems in the condensed phase with unprecedented accuracy, both in time and in space. We present results on the electronically excited high-spin state structure of an Fe(II) molecular species, $[Fe^{II}(bpy)_3]^{2+}$, in aqueous solution, resolving the Fe-N bond distance elongation as 0.2 Å. In addition an analysis technique using the reduced χ^2 goodness of fit between FEFF EXAFS simulations and the experimental transient absorption signal in energy space has been successfully tested as a function of excited state population and chemical shift, demonstrating its applicability in situations where the fractional excited state population cannot be determined through other measurements. Finally by using a novel ultrafast hard x-ray 'slicing' source the question of how the molecule relaxes after optical excitation has been successfully resolved using femtosecond XANES.

1. Introduction

X-ray absorption spectroscopy has proven to be an invaluable tool for measuring atomic-scale structures with sub-Å precision in disordered media. By introducing pump-probe techniques to the field of XAS [1, 2, 3] it has become possible to monitor both structural and electronic dynamics in systems as wide-ranging as solvated ions after photo-detachment of an electron [4, 5], through to the changes in local nuclear and electronic structure in transition metal-based molecular species [6, 7, 8, 9, 10, 11, 12], including the active centre in proteins after ligand detachment through optical excitation [13]. By taking advantage of the native pulsed x-ray timing structure available at 3^{rd}-generation synchrotron sources we have the ability to probe species in solution on the sub-100 picosecond (ps) timescale which has allowed us to investigate long-lived electronic excitation in molecules, using the power of EXAFS and XANES to resolve

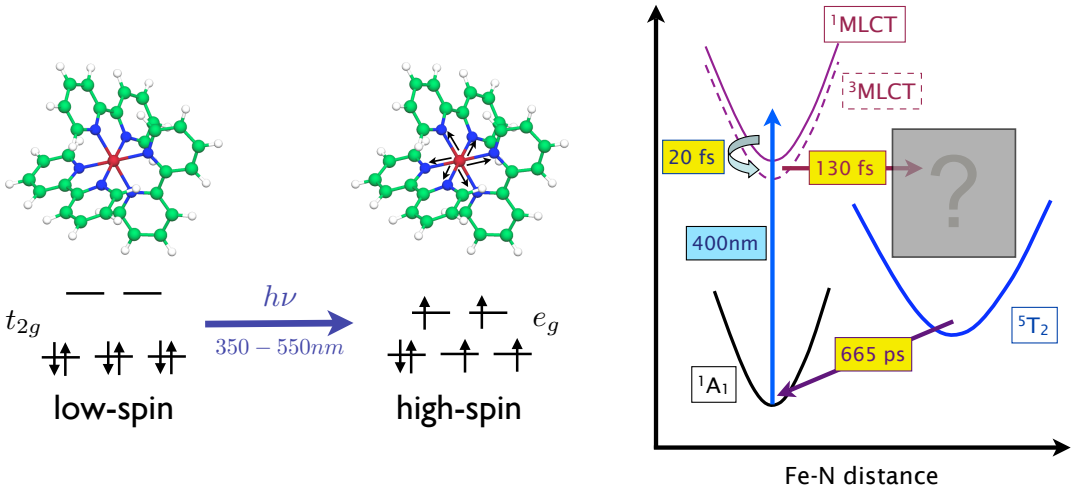

Figure 1. Spin-crossover transition in $[Fe^{II}(bpy)_3]^{2+}$ upon excitation with visible light. Left: molecular structure and spin-state change upon excitation from the low-spin (Fe-N bonding) to the high-spin (Fe-N antibonding) configuration. Right: Energy level diagram summarizing laser-only optical results.[23]

short-lived atomic and molecular excited states in solution [8, 10, 4, 11]. Recently we have used the novel x-ray-laser slicing technique [14], available at very few synchrotrons around the world [15, 16, 17], to observe dynamics on the femtosecond (fs) timescale, the fundamental timescale of nuclear motion. This has allowed us to observe the energy relaxation pathway of a spin-crossover molecular system in solution by fs XANES, resolving for the first time the question of how the molecule relaxes to the high-spin state after the initial optical excitation step [18]. A critical requirement for the analysis of such signals is the excited state population which is necessary to quantitatively disentangle the ground-state spectrum from the excited-state spectrum in the experimental signal [2]. Until recently it was necessary to obtain this information from laser-only spectroscopic measurements which, when not readily available, made analysis both more difficult and more inaccurate. By introducing the excitation population percentage as a parameter in the goodness of fit (χ^2) between the experiment and iterative FEFF simulations [19, 20, 21] in energy space it has become possible to obtain very accurately the excited state spectrum without any *a priori* knowledge of the excitation percentage. By applying this technique to a measurement where the excitation population was measured using other methods it has been possible to confirm its applicability and robustness [22], adding another analysis tool to the arsenal of experimental time-resolved x-ray spectroscopists.

2. Background

When a transition metal ion, such as Fe^{2+}, is placed in an octahedral crystal field its d-orbitals are split by the ligand-field interaction [24], giving rise to the well-known e_g and t_{2g} orbitals. When filling the orbitals with electrons the splitting, or 10Dq, determines whether the system is in a low-spin (LS) or high-spin (HS) configuration from the electron pairing. Transitions between the LS and HS states can be induced using temperature, pressure or visible light. In some cases, where the splitting is small, the molecule can be trapped in either the LS or HS state, allowing static measurements to be made on the system. $[Fe^{II}(bpy)_3]^{2+}$ is an example of a spin-crossover molecular system where the ground-state is the low-spin configuration, and the transition to the high-spin state can only be induced with visible light due to the large

energy difference between the LS and HS states [25] (see Figure 1). For this particular molecule the initial excitation is from a singlet ground state ($^1A_1$) to a singlet metal-to-ligand charge transfer state (^{1}MLCT). From fluorescence up-conversion measurements it is possible to resolve the very fast singlet to triplet energy transfer (^{1}MLCT $\rightarrow$ ^{3}MLCT) which occurs within 20 fs, quickly followed by a relaxation out of the ^{3}MLCT within 130-150 fs [26]. From this point in the energy relaxation pathway there is no way of following the dynamics by spectroscopy because all steps are silent. Ultrafast transient absorption measurements confirm the measurements made by McCusker and co-workers [25] showing a ground-state recovery of 665 ps as the high-spin state ($^5T_2$) relaxes back to the $^1A_1$ ground state. Two unresolved questions are: 1) what is the structure of the excited HS state? and 2) what is the relaxation pathway from the ^{3}MLCT to the HS state? Clearly time-resolved XAS is ideal to resolve structural questions, but can we also probe the system at shorter timescales and extract meaningful information to address the relaxation pathway?

3. Experimental Techniques

A short description of the techniques used follows. For further details please see references [1, 2, 27, 28] and references therein.

3.1. Beamline details

All experiments described here were performed at the MicroXAS beamline at the Swiss Light Source (SLS) which is located at the Paul Scherrer Institut (PSI). The SLS is a 3^{rd}-generation 2.4 GeV synchrotron which operates at a ring current of 400 mA and uses top-up mode to ensure a constant flux of x-rays. The beamline consists of an in-vacuum undulator capable of generating x-rays from 4-20 keV with a flux of approximately 10^{12} photons/second/0.015% BW (400 mA ring current). The photons are collected with a 1 m long Rh-coated, grazing incidence toroidal mirror (M1) capable of vertical collimation and limited horizontal focussing. The beamline is equipped with double-crystal, fixed exit monochromator containing Si(111), Ge(111) and Si(311) crystals to provide a range of x-ray energy resolutions. Immediately before the experimental endstation are a pair of Kirkpatrick-Baez (KB) micro-focussing mirrors, capable of focussing the x-ray flux down to a 1x1 μm^2 focal spot.

3.2. Pump-probe excitation and data acquisition

The pump-probe technique involves excitation of the sample with a short laser pulse, followed by a variable time delay after which the sample is probed with a short x-ray pulse. The XAS signal is generally measured simultaneously in both transmission and fluorescence using large area fast avalanche photodiodes in order to be able to electronically select only the x-rays from the isolated probe pulse using boxcar integrators. By using a fast data acquisition scheme that alternates between the XAS signal measured from the excited sample at a specific x-ray energy and laser/x-ray relative delay time, followed 500 μs later by the same XAS measurement of the unexcited sample, it is possible to achieve shot-noise limited measurements where the noise is thus derived solely from the photon statistics of the x-ray source [29]. Where possible an I_{zero} measurement is performed giving us the ability to normalize out incoming x-ray fluctuations due to monochromator imperfections and sudden increases in x-ray signal due to top-up injections. In general the transient absorption signals measured are: $T_{tr} = \ln(I_{tr}^{unp}/I_{tr}^{pu})$ for transmission and $T_{fluo} = (I_{fluo}^{pu} - I_{fluo}^{unp})/I_{zero}$ for fluorescence [28], where *pu* indicates the pumped or excited sample while *unp* indicates the unpumped or ground-state sample.

3.3. Ultrafast optical and x-ray pulses

The achievable time-resolution of the experiment is generally determined by the cross-correlation of the excitation laser pulse and the probing x-ray pulse. The stability of these sources, in pulse

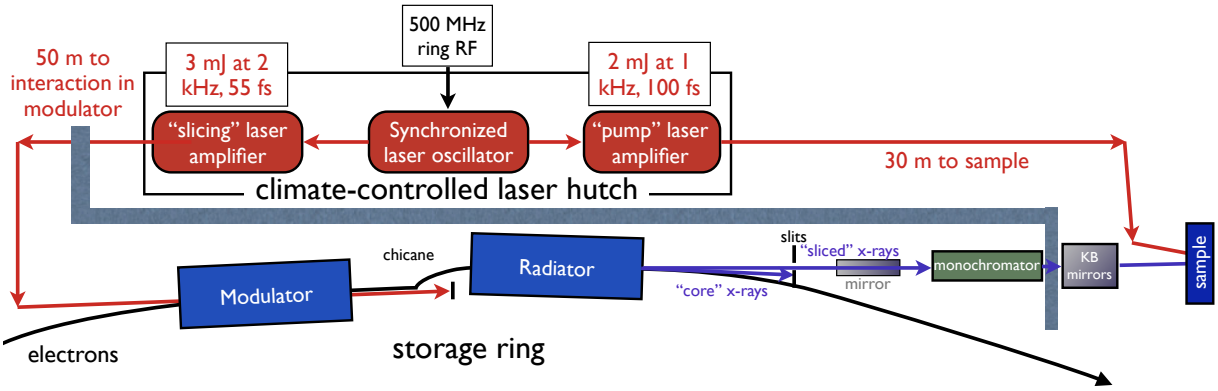

Figure 2. Layout of "pump" laser and "slicing" laser at the MicroXAS beamline (Swiss Light Source)

energy and in timing jitter, is critically important as we are performing XAS measurements over days or even weeks. In addition it is also vital to have excellent mechanical and electronic stability of all components in order to achieve the signal-to-noise necessary for our excited-state analyses.

Excitation laser The excitation laser source starts with a 100 MHz laser oscillator which is synchronized to the 500 MHz RF signal from the synchrotron ring with <1 ps of timing jitter. This synchronization is maintained with a Femtolock feedback system over the duration of our experiments which are generally over several weeks. A portion of the oscillator output is then regeneratively amplified to produce 100 fs, 800 nm laser pulses with 2 mJ of pulse energy at a repetition rate of 1 kHz. The laser is then transported from the temperature and humidity controlled laser hutch to the x-ray experimental hutch through a 30 m long evacuated transfer line. These laser pulses can then be converted to the excitation wavelength of interest using either doubling (400 nm), tripling (266 nm) or optical parametric amplification (tuneable between 250 - 2000 nm).

Picosecond x-rays The native timing structure of the electron bunches in the Swiss Light Source allows for an isolated single bunch to be placed at the end of the fill pattern within an electron-free gap of 170 nanoseconds. This hybrid bunch, also called the camshaft, has a duration of around 100 ps depending on the current in the bunch which is usually maintained at 4 mA. By precisely controlling the electronic timing between the 500 MHz RF signal of the ring and the synchronized laser oscillator it is possible to perform pump-probe measurements with <1 ps of timing jitter between the excitation laser and the probing x-ray pulse. By shifting the phase of the oscillator RF synchronization signal it is possible to vary the time delay between laser and x-rays. On average we obtain 10^3-10^4 photons/pulse depending on x-ray energy and focussing conditions.

Femtosecond x-rays First proposed in 1996 by Zholents and Zolotorev [14] and demonstrated at the Advanced Light Source by Schoenlein and co-workers in 2000 [15], the x-ray-laser slicing technique is now the established method to extract fs x-rays pulses at synchrotrons [15, 16, 17]. The technique involves spatial and temporal overlap of an intense fs laser pulse with the hybrid electron bunch in the storage ring within a wiggler (modulator) which is designed to optimize the electron-laser interaction (see Figure 2). The FEMTO slicing source at the Swiss Light

Source [17] starts by using a portion of the same synchronized laser oscillator output as the excitation laser, which ensures inherent fs synchronization between the pump laser and the probing 'sliced' x-rays. This seed pulse is then regeneratively amplified before passing through a double-pass cryo-cooled Titanium:Sapphire amplifier crystal pumped with two 30 W green lasers which amplifies the laser pulse up to 3 mJ/pulse at a repetition rate of 2 kHz. The pulse is then compressed to 55 fs duration (FWHM) using large area gratings before being gently focussed down to approximately 1 mm^2 over the 50 m distance to the interaction point within the modulator in the storage ring. The interaction between the laser electric field and the electron bunch results in an increased energy spread in the electrons. Immediately after the modulator the electrons pass through a dipole chicane which horizontally separates out the energy-modulated fs electrons from the core 100 ps bunch. Finally the electrons pass through the MicroXAS undulator (radiator) generating x-rays. By inserting a diaphragm at the beginning of the beamline most of the 'core' x-rays can be blocked, allowing the fs x-rays to proceed through the beamline optics. The energy-modulation of the sliced hybrid bunch persists for several hundred ring round-trips after the slicing interaction resulting in a small amount of x-rays in each sliced pulse from the previous modulation. These x-rays, called the 'halo', are unavoidable and result in a ∼100 ps duration pedestal under the fs x-ray pulse. A final set of slits are spatially optimized immediately before the KB focussing mirrors to maximize the contrast between the sliced and halo x-rays. In order to estimate the contribution from the halo to the sliced flux we measure the 499^{th} round-trip halo after the slicing interaction, in other words the halo signal immediately preceding the next slicing event. This measurement can then be subtracted from the total flux to obtain the fs flux. The flux of these background x-rays contribute <10% to the overall x-ray flux in our measurements. As our detectors cannot distinguish between the fs (sliced) and ps (halo) x-rays it is important to be certain that any measured pump-probe signal stems solely from the fs x-rays. In order to ensure the halo x-rays do not contribute to the measured dynamics the time scans are limited to a short range of a few ps over which any pump-probe contribution from the halo x-rays will be negligible. For longer time scans, where the pump-probe delay starts to approach the timescale on which one can measure a signal using the 100 ps x-ray pulse (>15 ps), it is possible to change the laser timing to use the previous x-ray pulse as the probe and thus measure the ps signal contribution to the data and subtract it.

The slicing flux is around 10^5 photons/second/0.1% BW with an x-ray pulse duration of 140±30 fs with a timing stability with respect to the excitation laser of <30 fs rms over days of usage. In general when working under the same conditions as during picosecond experiments the slicing source generates the 3-orders of magnitude drop in photons/pulse one would expect when extracting a 55 fs slice from a 100 ps electron bunch. In addition to fs XAS measurements this source has also been used to perform fs x-ray diffraction measurements on bulk single crystals and thin films [17, 30, 31, 32].

3.4. Sample preparation and measurement details

In all cases liquid samples were used. The experiments used a high-speed liquid jet formed by using a gear pump to flow the sample through a thin slit in a sapphire nozzle, at a velocity sufficient to ensure fresh sample was probed by the x-rays for each shot. When properly optimized the laminar flow of the liquid surface was a few mm^2 with a thickness of 100 μm, providing a smooth liquid sheet of uniform thickness upon which to perform measurements. The samples were recirculated.

Aqueous $[Fe^{II}(bpy)_3]^{2+}$ Tris(2,2'-bipyridine)iron(II) chloride hexahydrate was used to prepare aqueous solutions of various concentrations using deionized water. Most measurements were performed with either 25 or 50 mM solutions. The sample was excited with 100 fs, 300 μJ

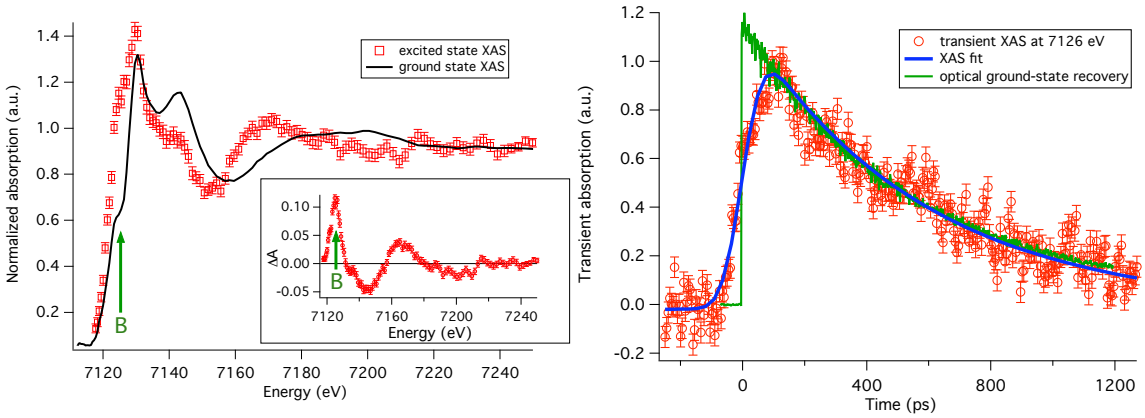

Figure 3. 25 mM aqueous $[Fe^{II}(bpy)_3]^{2+}$ ps data measured in both fluorescence and transmission. Left: XAS for the ground-state (black) and reconstructed excited-state 50 ps after excitation (red markers). The inset shows the transient difference spectrum with an arrow at the 'B' feature showing where the time scan is measured. Right: XAS time scan at 7126 eV (red markers) overlaid with the optical ground-state recovery signal (green curve) and a fit to the XAS signal (blue curve).

pulses of 400 nm light focussed to a spot size of 300 x 300 μm^2. The x-rays were tuned to the Fe K absorption edge (7.1 keV). The ps measurements [10] were performed with the Si(111) monochromator crystals with an energy resolution of 1 eV. The x-rays were focussed to a spot size of ~150 x 150 μm^2 spot using both KB mirrors. The fs measurements [18] were performed with the Ge(111) monochromator crystals, decreasing the energy resolution by a factor of two but commensurately increasing the number of x-rays per pulse by a factor of two. The x-rays were focussed using a single vertical KB mirror to 100 μm and horizontally using the M1 mirror to 250 μm. On average a flux of 10-15 photons/pulse was measured from the slicing source.

4. Results

The ps data for a 25 mM aqueous solution of $[Fe^{II}(bpy)_3]^{2+}$ is shown in Figure 3. The left side of Figure 3 shows the ground-state XAS signal and the reconstructed excited-state XAS signal, with the inset showing the transient absorption signal [28]. On the right side of Figure 3 is shown a time scan at the 'B' feature (7126 eV, red markers), the energy at which the maximum transient absorption signal occurs (green arrow in inset). Overlaid with this is the ground-state bleach recovery from laser-only measurements, confirming that what we are seeing is the relaxation from the HS excited state to the low-spin ground state with a decay time of 665 ps. By convolving a monoexponential fit curve with a decay constant of 650 ps with a 100 ps duration Gaussian x-ray probe pulse we obtain an excellent fit to the experimental result (blue curve in Figure 3). This indicates that the transient spectrum shown is a measurement of the molecule in the $^5T_2$ state and that the arrival time in this state is <50 ps..

Both MXAN simulations [33] and EXAFS analysis of the ground-state spectrum give an Fe-N bond distance of 2.00 ± 0.02Å, in excellent agreement with a crystallographic measurement of 1.967 ± 0.006Å[34] and DFT calculation result of 1.99 ± 0.02Å[35]. In general the transient energy spectrum can be defined as $\Delta A(E,t) = \sum_n f_n(t)\,[A_{ES_n}(E,t) - A_{GS}(E)]$ where the A_{ES} spectrum at time t will be composed of n different excited-state species. The excited state population at time t for each species requires that the total excitation must match the loss of

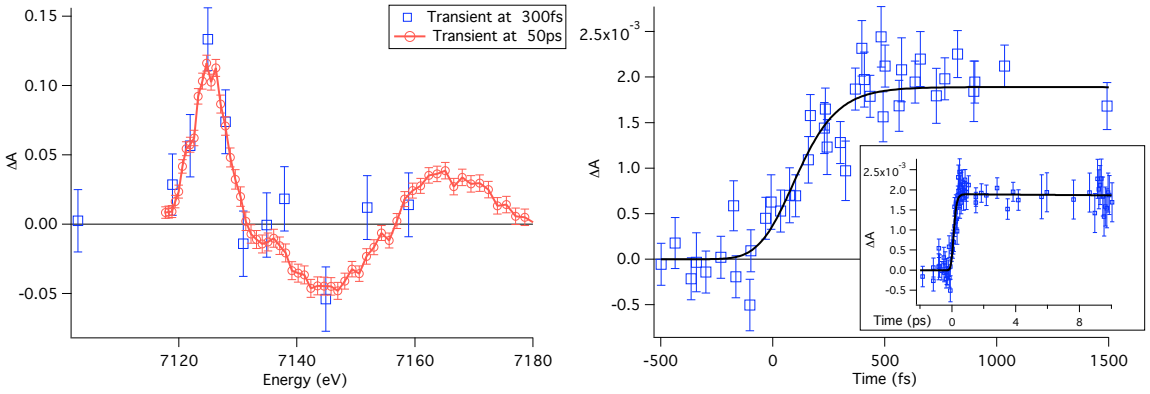

Figure 4. 50 mM aqueous $[Fe^{II}(bpy)_3]^{2+}$] fs data measured in transmission. Left: The transient signal measured at 50 ps (red markers) and at 300 fs (blue markers) with an arrow at 7126 eV showing where the time scans were performed. Right: Time scan performed at 7126 eV (blue markers) overlaid with a model allowing for an arrival in the high-spin state within 150 fs. Inset: Time scan data out to 10 ps.

ground state species: $\sum_n f_n(t) = f_{exc}(t)$. In the case of iron tris-bipyridine we expect to have contributions only from the HS state in the excited-state spectrum at $t = 50ps$. From laser-only optical measurements of the change in ground-state absorption we can estimate the excitation population to be $f_{exc}(50ps) = 22\% \pm 2\%$ [28], allowing us to obtain the excited-state spectrum shown on the left in Figure 3. From this it is possible to extract an Fe-N bond distance elongation of 0.2 Å. This represents the first *on-the-fly* measurement of the structure of a molecular system [10].

Turning now to the question of the relaxation cascade down to the HS state and given that the intermediate states are optically silent, fs XANES is ideal to determine the arrival time in the HS state. In addition the quality of the data measured for $[Fe^{II}(bpy)_3]^{2+}$ at 50ps shows that this molecule is a good candidate for measurement with the FEMTO slicing source. By taking advantage of the fact that we have a shot-noise limited detection system we can accurately predict the data accumulation times to obtain a reasonable signal-to-noise ratio using the slicing flux numbers compared to the ps flux numbers. The optimal conditions for measurement were determined to be a concentration of 50 mM, laser excitation conditions identical to those of the ps experiment, with the monochromator set to the maximum in the transient energy signal (the B feature at 7126 eV) to perform a time scan. Our multiple-scattering analysis also shows that the pre-edge shoulder, or 'B' feature, is sensitive to the Fe-N bond distance, with the absorption increasing as the bonds elongate. The results of this time scan are shown on the right side of Figure 4. We clearly see a very fast rise in the signal, reaching a plateau in <300 fs. This transient maximum matches the change in absorption at 50 ps, indicating we have reached the same change in absorption within 300 fs as at 50 ps. We then performed a transient energy scan at 300 fs, the result of which is shown on the left of Figure 4 (blue markers). Overlaid on top is the transient energy signal at 50 ps (red markers). Within the error bars it is clear that the two qualitatively and quantitatively match. From this we can conclude that we have reached the $^5T_2$ high-spin state within <300 fs. A fit of the time scan (blue trace in Figure 4) using a cross-correlation of 250 fs for the optical and x-ray pulses shows that the rise time is 150±50 fs. Therefore taking the information from the optical measurements we conclude that the process is a simple 4 step model: $^1A_1 \rightarrow {}^1$MLCT $\rightarrow {}^3$MLCT $\rightarrow {}^5T_2$, the result of which is shown as

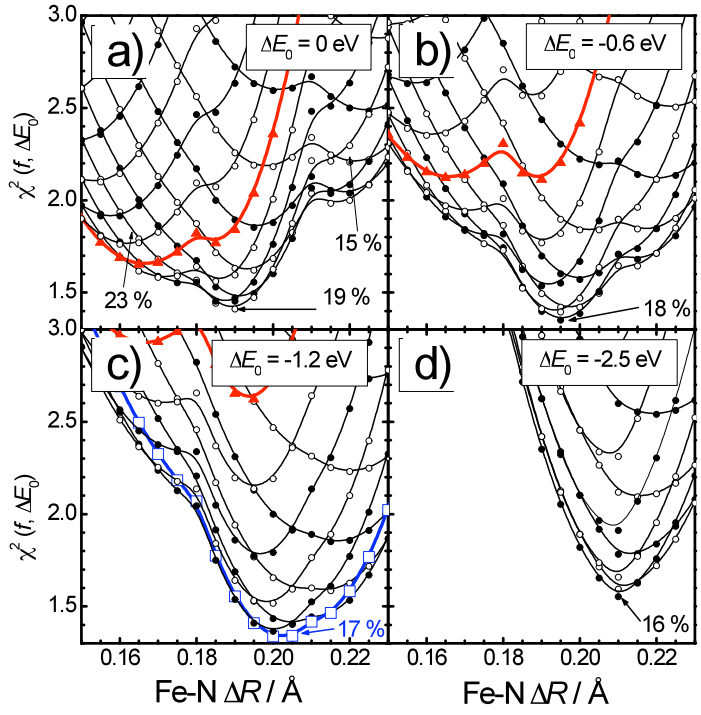

Figure 5. Result of residual χ^2 analysis described in text for an edge shift of (a) ΔE_0= 0 eV, (b) ΔE_0= -0.6 eV,(c) ΔE_0= -1.2 eV,(d) ΔE_0= -2.5 eV. The curves are guides to the eye and connect values with the same excitation (f). Red curves (triangles) in (a), (b) and (c) show an example calculation for an excitation of f=22%. Blue curve in (c) (open squares) shows the minimum value achieved for the residual χ^2 [22].

the black curve on the right side of Figure 4. What is immediately clear from this model is that there is no time for any other states to be involved in the relaxation pathway, indicating that the molecule proceeds directly from the ^{3}MLCT state to the high-spin $^5T_2$ state. This resolves the question of how $[Fe^{II}(bpy)_3]^{2+}$ relaxes to the high-spin state, a question which until now was the subject of speculation.

5. Analysis

The results shown here clearly indicate that we can successfully measure ultrafast transient XAS on both the ps and fs timescales. We have also demonstrated that the tools used for static XAFS analysis can also be used for our excited state measurements, with several restrictions. Two critical limitations are 1) the *a priori* knowledge of the excitation population contributing to the transient XAS signal and 2) the potential perturbation of the ionization energy (E_0), or chemical shift, in the molecule's excited state. In addition it would be substantially more accurate to take advantage of our sensitive transient absorption measurements in energy-space as opposed to the usual technique of back-Fourier transforming from the radial distribution function to obtain any structural changes. One approach which has used XAS to measure femtometer-scale changes due to magnetostriction is the DiffXAS technique of Pettifer, Ruffoni and co-workers [36, 37] where the differential EXAFS signal is fit to a first-order Taylor expansion of the EXAFS equation. This approach works well for small structural changes but cannot be generalized towards larger changes. The approach we have taken here is to start from a well-characterized ground-state structure and EXAFS spectrum, then using physically and chemically sensible changes, we modify the system to obtain the excited state. This can then be simulated using FEFF to obtain an EXAFS spectrum which can be used to generate a transient absorption signal to compare to experiment. The goodness of fit of this simulation to the experiment can be determined by calculating the reduced chi squared function but here we introduce other degrees of freedom, namely the excitation percentage (f) and the ionization energy shift for the excited

Table 1. Comparison of the Fe-N bond distances obtained from the various simulations

Fe-N(Å)	Error(Å)	f(%)	ΔE_0(eV)	Source
0.2	±0.02	22	-2.8±0.5	EXAFS analysis from [10]
0.19	±0.03	21.5±1.5	-2.5	MXAN analysis with fixed ΔE_0 [10]
0.2	±0.04	22	-2.5±0.5	MXAN analysis with fixed f [10]
0.203	-0.035, +0.012	22±1	-2.5±0.5	this analysis with f and ΔE_0 from Ref.[10]
0.2005	-0.0165,+0.0135	17±1	-1.2±0.6	this analysis 90% confidence levels [22]
0.203	±0.008	17±1	-1.2±0.6	this analysis 95% confidence levels [22]

state (ΔE_0):

$$\chi_r^2\left(i, f, \Delta E_0\right) = \frac{1}{(N-1)} \sum_{j=1}^{N} \left(\frac{x_j/f - \Delta A_j^i\left(\Delta R_i, \Delta E_0\right)}{\Delta x_j/f} \right)^2 \quad (1)$$

In Equation 1 we take the difference between the experimental result scaled with the excitation percentage (x_j/f) and the simulated transient (ΔA) for each point in energy space (j). This is then inversely weighted by the error of the experimental measurement also scaled with the excitation percentage ($\Delta x_j/f$). This sum then gives a representative number for how well the two transient absorption spectra match at a given excitation percentage. Since the simulated transient is a function of the energy shift between the ground and excited-state spectra, the reduced χ^2 is a function of the structural modifications (ΔR_i), the excitation percentage (f) and the energy shift (ΔE_0).

Before using this procedure generally it is important to establish its accuracy on a test case. As we know reasonably accurately the excitation percentage for the ps EXAFS $[Fe^{II}(bpy)_3]^{2+}$ measurement from optical measurements ($f = 22\% \pm 2\%$) and we have a reasonable value for the energy shift in the excited state from both MXAN simulation (-2.5 eV) and the transient EXAFS measurement (-2.8 eV±0.5 eV) [10] this is an ideal place to start. The results of the calculation for several examples are shown in Figure 5. Each point is a χ^2 value calculated for a specific excited state structural change, with a specific excitation population and a specific energy shift. The curves link together groups with the same excitation population. For example the red curves in Figure 5 (a), (b), (c) correspond to $f = 22\%$. Each of of the 4 plots shown correspond to a different value for ΔE_0. The structural modifications chosen were to vary the Fe-N bond distance while maintaining the structural integrity of the bipyridine ligands. By simply applying a blind change in Fe-N coordination sphere distance the result would have been a distorted bipyridine molecule, an unlikely occurrence due to the rigidity of the ligand structure. The result of this analysis procedure is an excitation population of $f = 17\% \pm 1\%$ with an energy shift of $\Delta E_0 = -1.2\text{eV} \pm 0.6\text{eV}$, resulting in a change in Fe-N bond distance of 0.203 ± 0.008Å within 95% confidence limits [22]. Further structural refinements, such as ligand distortion, are not feasible due to the experimental signal-to-noise. These values for f and ΔE_0 are similar to, but not the same as the previous measurement. The excitation yield difference is due to the fact that the optical measurement was performed with a 100 fs time resolution while the x-ray experiment was limited to 100 ps. The result of this is clear in the time scan on the right of Figure 3 where at 50 ps the x-ray signal has not reached its maximum value and is about 20% lower then the corresponding optical measurement. The result is a lower excitation population at 50 ps then estimated from the laser-only measurement by $\sim 20\%$, which

is approximately the difference between the 22% laser-only value and the 17% excitation obtained from the optimization procedure. The ΔE_0 difference is not as easily explained. Subsequent analysis shows that the Fe-N bond distance obtained is relatively insensitive to the energy shift used (see Table 1). The reduced χ^2 value is, however, very sensitive to changes in f and ΔE_0, making it perhaps a more accurate method then previous techniques. The value obtained from the reduced χ^2 procedure is comparable to the 10Dq splitting of 1.6 eV obtained for $[Fe^{II}(bpy)_3]^{2+}$ [38], indicating that -1.2 eV is a reasonable number to expect for the energy shift. From our analysis it is clear that the excited state structure can be obtained as a function of both the excitation population and the energy shift with reasonable accuracy without any *a priori* knowledge. This conclusion has subsequently been successfully tested with a phosphorescent di-platinum complex where no optical excitation population measurement was possible, resulting in an accurate structural analysis of the excited state [11].

6. Conclusions

Time-resolved XAS is a new and growing field that has the potential to revolutionize our knowledge of structure and dynamics. The ability to probe the local structure of systems in solution is unique and provides us with an unprecedented view on how molecular systems behave on ultrafast timescales. Of paramount importance is the ability to reach the femtosecond regime where the fundamental timescales of nuclear dynamics become accessible. This relevance is demonstrated by our measurement of the fs XANES spectrum of the spin-crossover complex $[Fe^{II}(bpy)_3]^{2+}$ where this technique has resolved the question of how the molecule relaxes from the initial excitation through to the high-spin state. One of the key requirements to taking advantage of these techniques at 4^{th}-generation XFELs, where one second's worth of x-ray flux at current x-ray sources will be contained in a single fs pulse, is the ability to simulate and analyze the experimental signals. Though some progress has been made in this area, for example the reduced χ^2 technique mentioned here [22, 11] and the DiffXAS technique [36, 37], there is still a long way to go before such analysis becomes routine. This is a challenging prospect, but one which is worth the effort as the ability to resolve molecular dynamics with sub-Å precision has the power to advance our understanding across all fields of science.

References

[1] Bressler C and Chergui M 2004 *Chem Rev* **104** 1781–1812
[2] Bressler C, Abela R and Chergui M 2008 *Z Kristallogr* **223** 307–321
[3] Chergui M and Zewail A H 2009 *ChemPhysChem* **10** 28–43
[4] Pham V T, Gawelda W, Zaushitsyn Y, Kaiser M, Grolimund D, Johnson S L, Abela R, Bressler C and Chergui M 2007 *J Am Chem Soc* **129** 1530–1531
[5] Elles C G, Shkrob I A, Crowell R A, Arms D A and Landahl E C 2008 *J Chem Phys* **128** 061102
[6] Thiel D, Livins P, Stern E and Lewis A 1993 *Nature* **362** 40–43
[7] Chen L, Jager W, Jennings G, Gosztola D, Munkholm A and Hessler J 2001 *Science* **292** 262–264
[8] Saes M, Bressler C, Abela R, Grolimund D, Johnson S L, Heimann P A and Chergui M 2003 *Phys. Rev. Lett.* **90** 047403
[9] Khalil M, Marcus M A, Smeigh A L, McCusker J, Chong H H W and Schoenlein R W 2006 *J Phys Chem A* **110** 38–44
[10] Gawelda W, Pham V T, Benfatto M, Zaushitsyn Y, Kaiser M, Grolimund D, Johnson S L, Abela R, Hauser A, Bressler C and Chergui M 2007 *Phys. Rev. Lett.* **98** 4
[11] van der Veen R, Milne C J, Nahhas A E, Lima F, Pham V T, Best J, Weinstein J, Borca C, Abela R, Bressler C and Chergui M 2009 *Angew. Chem. Int. Ed.* **48** 2711–2714
[12] Huse N, Khalil M, Kim T K, Smeigh A L, Jamula L, Mccusker J K and Schoenlein R W 2009 *J. Phys.: Conf. Ser.* **148** 012043
[13] Wang H, Peng G and Cramer S 2005 *J Electron Spectrosc* **143** 1–7
[14] Zholents A and Zolotorev M S 1996 *Phys. Rev. Lett.* **76** 912–915
[15] Schoenlein R W, Chattopadhyay S, Chong H H W, Glover T E, Heimann P A, Shank C V, Zholents A A and Zolotorev M S 2000 *Science* **287** 2237–2240

[16] Khan S, Holldack K, Kachel T, Mitzner R and Quast T 2006 *Phys. Rev. Lett.* **97** 074801
[17] Beaud P, Johnson S L, Streun A, Abela R, Abramsohn D, Grolimund D, Krasniqi F, Schmidt T, Schlott V and Ingold G 2007 *Phys. Rev. Lett.* **99** 174801
[18] Bressler C, Milne C J, Pham V T, Nahhas A E, Veen R M V D, Gawelda W, Johnson S, Beaud P, Grolimund D, Kaiser M, Borca C N, Ingold G, Abela R and Chergui M 2009 *Science* **323** 489–492
[19] Rehr J and Albers R 2000 *Rev Mod Phys* **72** 621–654
[20] Newville M 2001 *J Synchrotron Rad* **8** 322–324
[21] Ravel B and Newville M 2005 *J Synchrotron Rad* **12** 537–541
[22] Gawelda W, Pham V T, Veen R M V D, Grolimund D, Abela R, Chergui M and Bressler C 2009 *J Chem Phys* **130** 124520
[23] Gawelda W, Johnson M, de Groot F, Abela R, Bressler C and Chergui M 2006 *J Am Chem Soc* **128** 5001–5009
[24] Hauser A, Enachescu C, Daku M, Vargas A and Amstutz N 2006 *Coordination Chemistry Reviews* **250** 1642–1652
[25] McCusker J, Walda K, Dunn R, Simon J, Magde D and Hendrickson D 1993 *J Am Chem Soc* **115** 298–307
[26] Gawelda W, Cannizzo A, Pham V T, van Mourik F, Bressler C and Chergui M 2007 *J Am Chem Soc* **129** 8199–8206
[27] Saes M, Bressler C, van Mourik F, Gawelda W, Kaiser M, Chergui M, Bressler C, Grolimund D, Abela R, Glover T, Heimann P, Schoenlein R, Johnson S, Lindenberg A and Falcone R 2004 *Rev Sci Instrum* **75** 24–30
[28] Gawelda W 2006 *Time-resolved x-ray absorption spectroscopy of transition metal complexes* Ph.D. thesis Ecole Polytechnique Fédérale de Lausanne
[29] Gawelda W, Pham V T, Nahhas A E, Kaiser M, Zaushitsyn Y, Johnson S L, Grolimund D, Abela R, Hauser A, Bressler C and Chergui M 2007 *AIP Conference Proceedings* **882** 31–36
[30] Johnson S L, Beaud P, Milne C J, Krasniqi F S, Zijlstra E S, Garcia M E, Kaiser M, Grolimund D, Abela R and Ingold G 2008 *Phys. Rev. Lett.* **100** 155501
[31] Johnson S L, Beaud P, Vorobeva E, Milne C J, Murray E D, Fahy S and Ingold G 2009 *Phys. Rev. Lett.* **102** 175503
[32] Krasniqi F S, Johnson S L, Beaud P, Kaiser M, Grolimund D and Ingold G 2008 *Phys. Rev. B* **78** 174302
[33] Benfatto M, Longa S D, Hatada K, Hayakawa K, Gawelda W, Bressler C and Chergui M 2006 *J Phys Chem B* **110** 14035–14039
[34] Dick S 1998 *Z Krist-New Cryst St* **213** 356–356
[35] Daku L, Vargas A, Hauser A, Fouqueau A and Casida M 2005 *Chemphyschem* **6** 1393–1410
[36] Pettifer R, Mathon O, Pascarelli S, Cooke M and Gibbs M 2005 *Nature* **435** 78–81
[37] Ruffoni M P, Pascarelli S, Groessinger R, Turtelli R S, Bormio-Nunes C and Pettifer R F 2008 *Phys. Rev. Lett.* **101** 147202
[38] de Groot F 2005 *Coordination Chemistry Reviews* **249** 31–63